30 p.

ELECTRO-OPTICAL SYSTEMS, INC., Pasadena, California

HYDROGEN-OXYGEN ELECTROLYTIC REGENERATIVE FUEL CELLS

Prepared for

National Aeronautics and Space Administration
Lewis Research Center
21000 Brookpark Road
Cleveland 35, Ohio
Attn: D.G. Soltis

Contract NAS 3-2781

EOS Report 4110-QL-2

18 January 1964

Prepared by

Harvey Frank

Harvey Frank
Project Supervisor

Approved by:

E. Findl
Manager
Chemical and Fluid Systems

A. R. Tanguay
Manager
Energy Conversion Div.

ELECTRO-OPTICAL SYSTEMS, INC.

Pasadena, California

TABLE OF CONTENTS

LIST OF ILLUSTRATIONS

I. INTRODUCTION

The objective of this program is to evaluate rechargeable hydrogen-oxygen fuel cells for orbital applications. Such cells are proposed as energy storage devices in conjunction with silicon solar cell converters. The important advantages of hydrogen-oxygen cells over existing energy storage devices are that they exhibit higher energy to weight ratios, can operate over higher operating temperature limits, contain a state of charge indicator, and have potentially longer cycle life. The particular design concept employed on this program utilizes isothermal operation with no moving parts, and therefore places no additional heating load on a vehicle's cooling system.

The initial phase of this program was concerned with an analytical determination of the performance of a complete power system which contained a fuel cell as the energy storage device. The overall, as well as component weights of this system, were determined as functions of the orbital altitude and power level.

The second phase of this program was to design and fabricate a 75 watt (nominal) fuel cell having features suitable for later scale up. The final phase of the program consists of testing and evaluating the 75 watt battery in order to determine its operational characteristics.

15534 over

2. SUMMARY

The major accomplishments during the past quarter were concerned with the development of the 75 watt model and associated control apparatus to simulate orbital cycling. After several modifications of the initial assembly were made, its design was finalized and fabrication of the component parts was initiated. Machining of these parts was completed during the latter portion of the quarter at which time they were sent out for electroless nickel plating. The plating will be completed in the early portion of the third quarter at which time the unit will be assembled and given preliminary check out tests.

Development of the control and recording apparatus for continuous cycling was completed during the latter portion of the quarter. The unit was tested and found to function satisfactorily. The unit will control and record the charge-discharge current and time for the specified cycle conditions. The unit will also record the overall and individual cell voltages, cell temperatures, and gas pressures.

Voltage-current and cycle tests were carried out on simulated single cells of the final assembly. One such cell with 5.8 inch diameter electrodes delivered 25.4 amps (148 m.a./cm^2) at 0.74 volts with gas pressures of 100 psig and temperature near 70°C. A smaller cell with 2 1/2 inch diameter electrodes was carried through complete charge-discharge cycles under similar conditions. The charge voltage for the smaller cell was 1.5 volts at 53 m.a./cm^2, and the discharge voltage an average of 0.8 volts for the major portion of the discharge period at a current of 104 m.a./cm^2. These results indicate that the design goals of the 75 watt prototype are realistic.

15534

Heat generation and heat transfer analyses were carried out on the prototype model. The results indicate a heat generation rate of about 80 watts for discharge at 19 amps, and essentially zero watts during charge at 70°C. The estimated heat transfer rate by external natural convection is 52 watts and the heat transfer rate by radiation is in the range of 10 to 60 watts depending upon the emissivity of the surface. These results indicate the necessity of providing insulation or an external heat source for ambient testing in order to maintain a temperature of 70°C.

Corrosion tests were carried out on samples of nickel plated magnesium and aluminum. The results indicate the suitability of a 3 mil layer of electroless nickel in regard to protection of the metal substrate against attack by the KOH electrolyte and oxygen within the cell.

AUTHOR

3. TECHNICAL DISCUSSION

This section outlines the progress made in the development of the six cell prototype with associated control equipment, and also reviews the results of supporting developmental studies.

3.1 Prototype Development

The developmental status of the prototype and control equipment are described below.

3.1.1 Fuel Cell Assembly

The first design of the prototype was completed in November, 1963, and was reviewed at that time with the technical monitor. Minor modifications were subsequently made (see below) and the design was finalized. Fabrication of the component parts was completed in the first week of January, 1964, at which time they were inspected and then sent out for nickel plating. The nickel plating is required to prevent chemical and electrochemical attack of the materials of construction, i.e., magnesium and aluminum, by the strong basic electrolyte (35% potassium hydroxide solution). A coating of 3 mils of nickel will be applied by the Kanigen electroless nickel process. The parts will be ready for assembly in mid January, 1964.

The modifications of the first design (see Fig. 1) were made in order to improve reliability, and to simplify fabrication. The first such modification consisted of a slight increase in the diameter of the cell separators in order to provide more sealing area for the teflon gaskets. A second modification consisted of increasing the thickness of the separators in order to simplify the machining of the inlet radial holes which serve as gas ports. A third and final

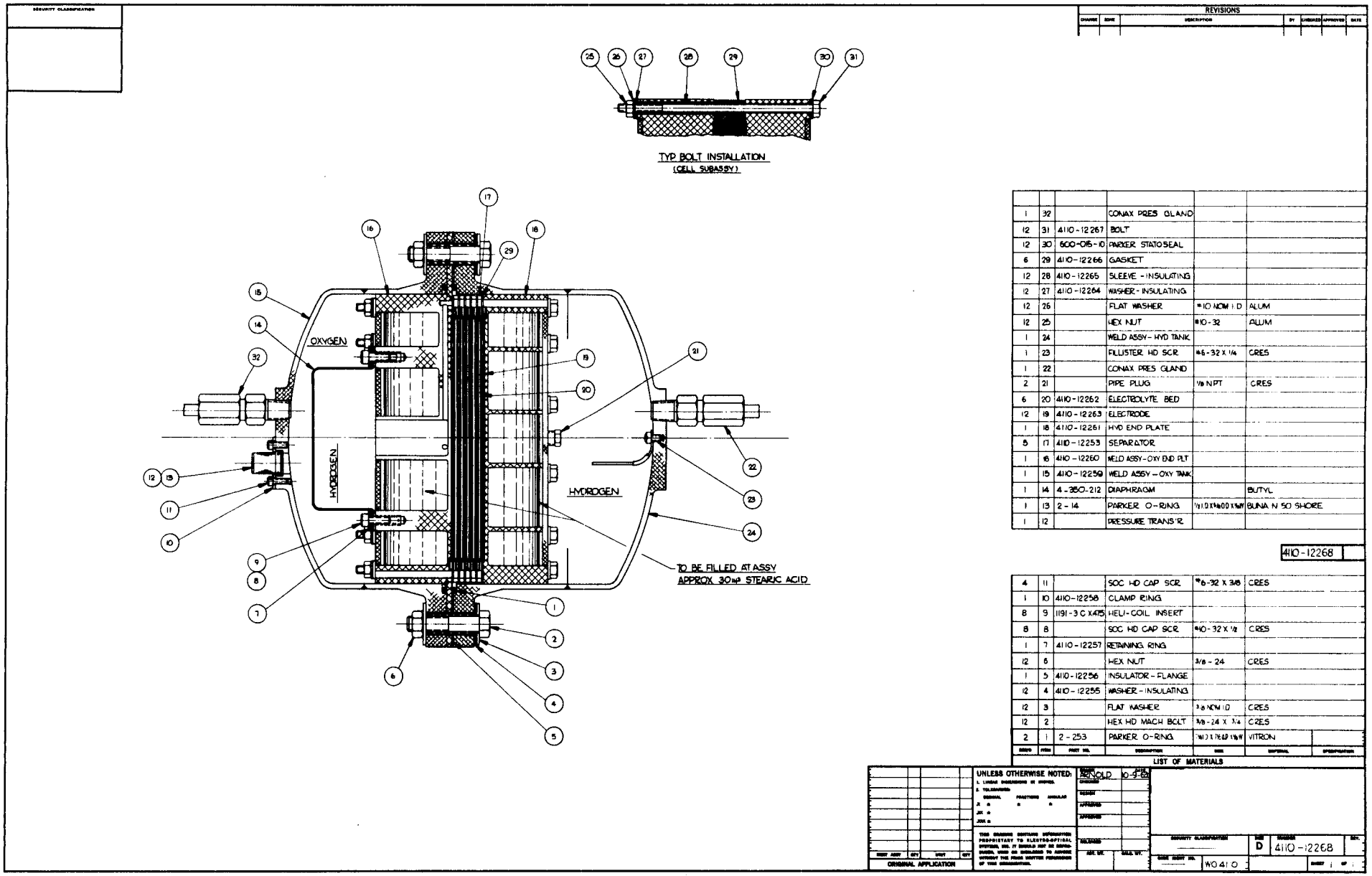

1	32		CONAX PRES GLAND		
12	31	4110-12267	BOLT		
12	30	600-015-10	PARKER STATO SEAL		
6	29	4110-12266	GASKET		
12	28	4110-12265	SLEEVE - INSULATING		
12	27	4110-12264	WASHER - INSULATING		
12	26		FLAT WASHER	#10 NOM I.D	ALUM
12	25		HEX NUT	#10-32	ALUM
1	24		WELD ASSY - HYD TANK		
1	23		FILLISTER HD SCR	#6-32 X 1/4	CRES
1	22		CONAX PRES GLAND		
2	21		PIPE PLUG	1/8 NPT	CRES
6	20	4110-12262	ELECTROLYTE BED		
12	19	4110-12263	ELECTRODE		
1	18	4110-12261	HYD END PLATE		
5	17	4110-12253	SEPARATOR		
1	16	4110-12260	WELD ASSY-OXY END PLT		
1	15	4110-12259	WELD ASSY - OXY TANK		
1	14	4-350-212	DIAPHRAGM		BUTYL
1	13	2-14	PARKER O-RING	1/2 I.D X 9/16 O.D X 1/16 W	BUNA N 50 SHORE
1	12		PRESSURE TRANS'R		

4110-12268

4	11		SOC HD CAP SCR	#6-32 X 3/8	CRES
1	10	4110-12258	CLAMP RING		
8	9	1191-3 C X.475	HELI-COIL INSERT		
8	8		SOC HD CAP SCR	#10-32 X 1/2	CRES
1	7	4110-12257	RETAINING RING		
12	6		HEX NUT	3/8-24	CRES
1	5	4110-12256	INSULATOR - FLANGE		
12	4	4110-12255	WASHER - INSULATING		
12	3		FLAT WASHER	3/8 NOM I.D	CRES
12	2		HEX HD MACH BOLT	3/8-24 X 3/4	CRES
2	1	2-253	PARKER O-RING	7/8 I.D X 1/16 O.D X 1/16 W	VITRON

LIST OF MATERIALS

UNLESS OTHERWISE NOTED:

ORIGINAL APPLICATION

D 4110-12268

WO 41 0

FIG. 1 FUEL CELL ASSEMBLY

modification consisted of the elimination of the concentric grooves on the surfaces of the separators which serve to distribute the inlet gases to the electrodes. In place of the grooves, it was decided to employ fine mesh nickel screens to aid in the gas distribution. The reason for the latter change was to simplify the machining operation. Resulting dimensional changes of all other parts were also made to compensate for the above modifications. Photographs of the cell and its components are shown on Figures 2 through 4.

Although the above changes will slightly increase the size and weight of the assembly, they will not appreciably affect the overall configuration or anticipated performance. The unit will contain six series connected cells. The electrode diameter of the cells are 6 inches. Gas containers having a volume ratio of 2/1 respectively for hydrogen and oxygen are integral, and are of such size that the maximum gas pressure will be $\approx$ 400 psig at the full state of charge. It is anticipated that the nominal 75 watt output will be achieved at voltages approaching 5 volts. The unit will, however, be carried through the previously planned cycle conditions consisting of a charge at 9.6 amps for 76 minutes and discharge at 19 amps for 37.5 minutes.

Instrumentation of the unit will include measurement of individual cell voltage and temperature, overall battery voltage and current as well as gas pressure and surface temperature.

Preparation of the required number of electrodes, nickel screens, and electrolyte beds has been completed, and these parts are ready for assembly. The hydrogen electrodes contain a mixture of 5 mg/cm^2 of platinum and 5 mg. palladium/cm^2, and the oxygen electrodes contain 10 mg platinum/cm^2. The electrolyte beds will have an electrolyte content of 0.7 gms of 35 percent KOH solution per gram of dry asbestos.

3.1.2 Control Apparatus

Development of the control apparatus for continuous cycling was completed during this report period. A schematic diagram of the apparatus is given in figure 5. The unit can be connected to

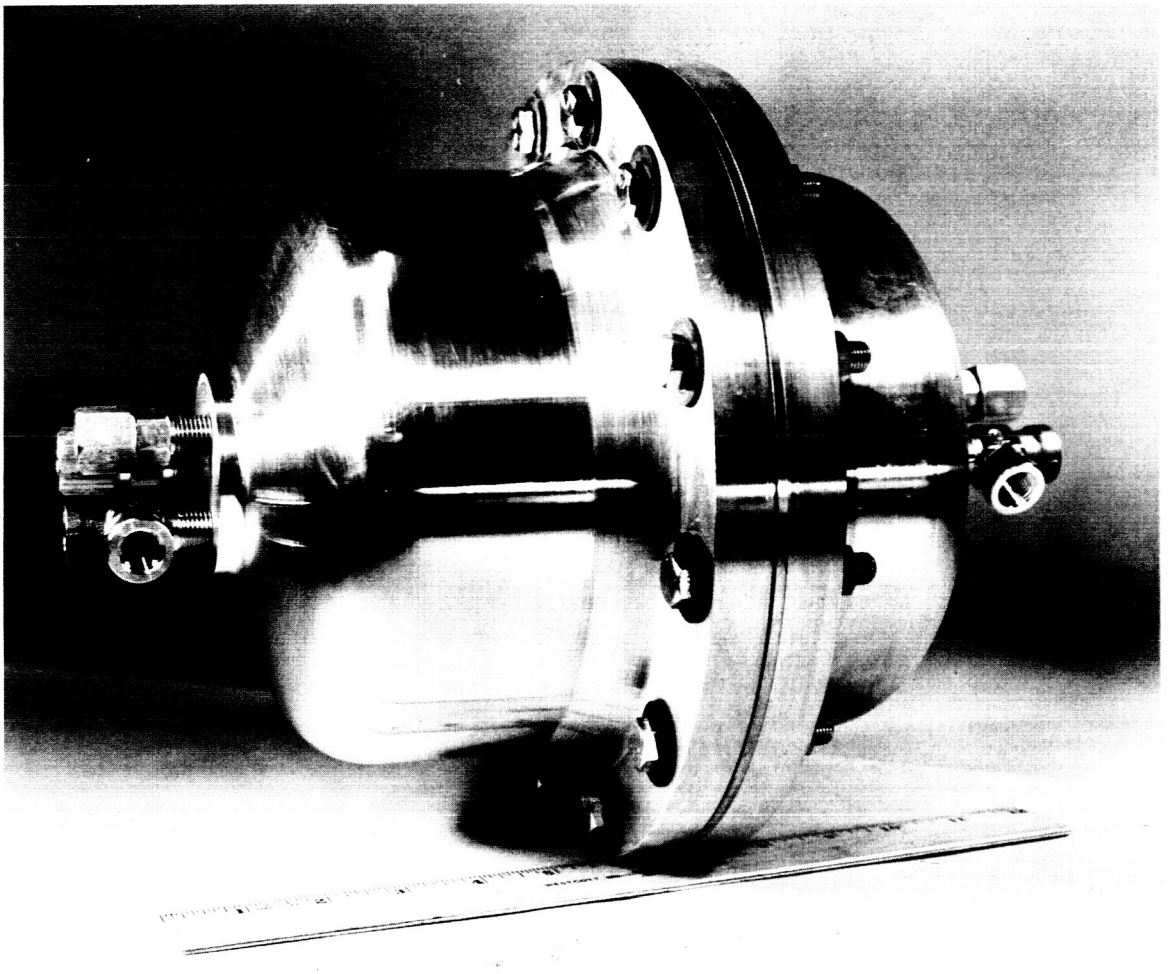

FIG. 2 FUEL CELL ASSEMBLY

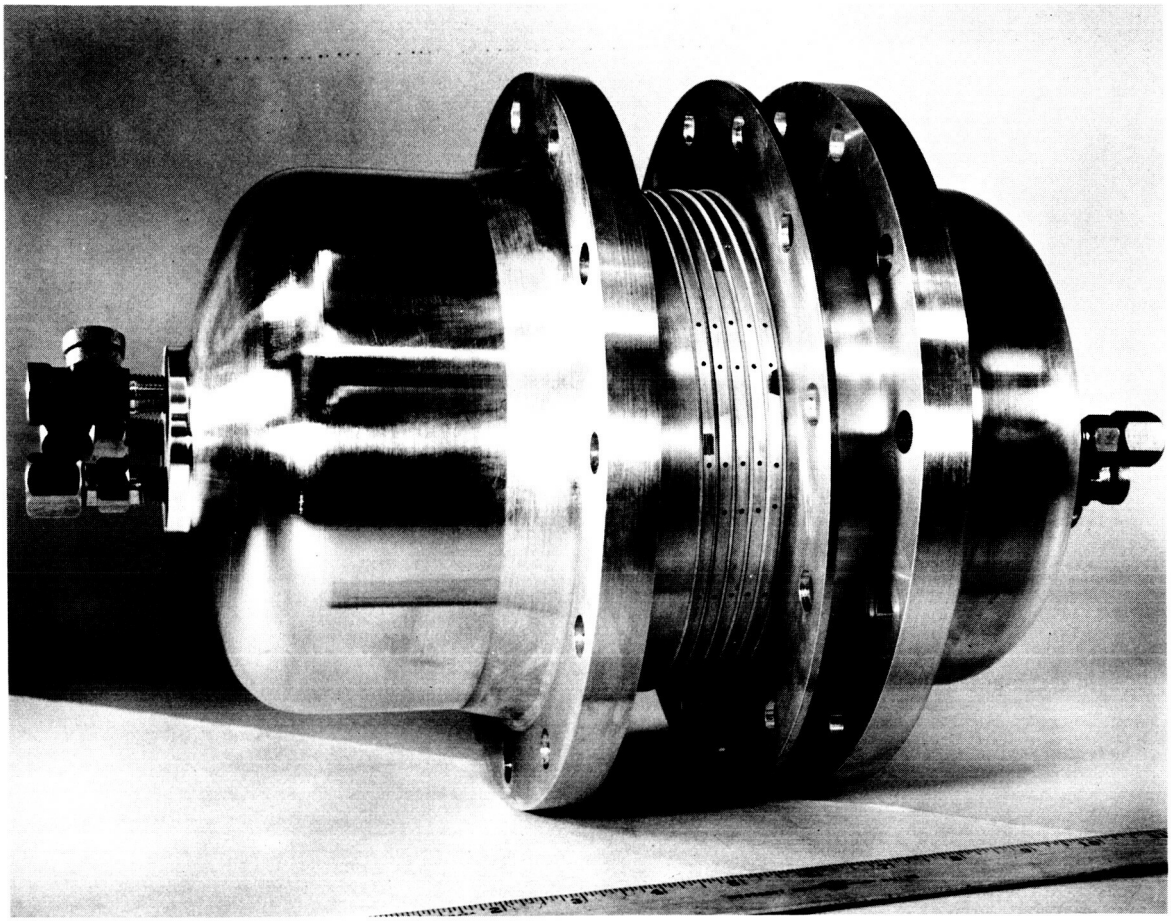

FIG. 3 FUEL CELL ASSEMBLY PARTIALLY DISASSEMBLED

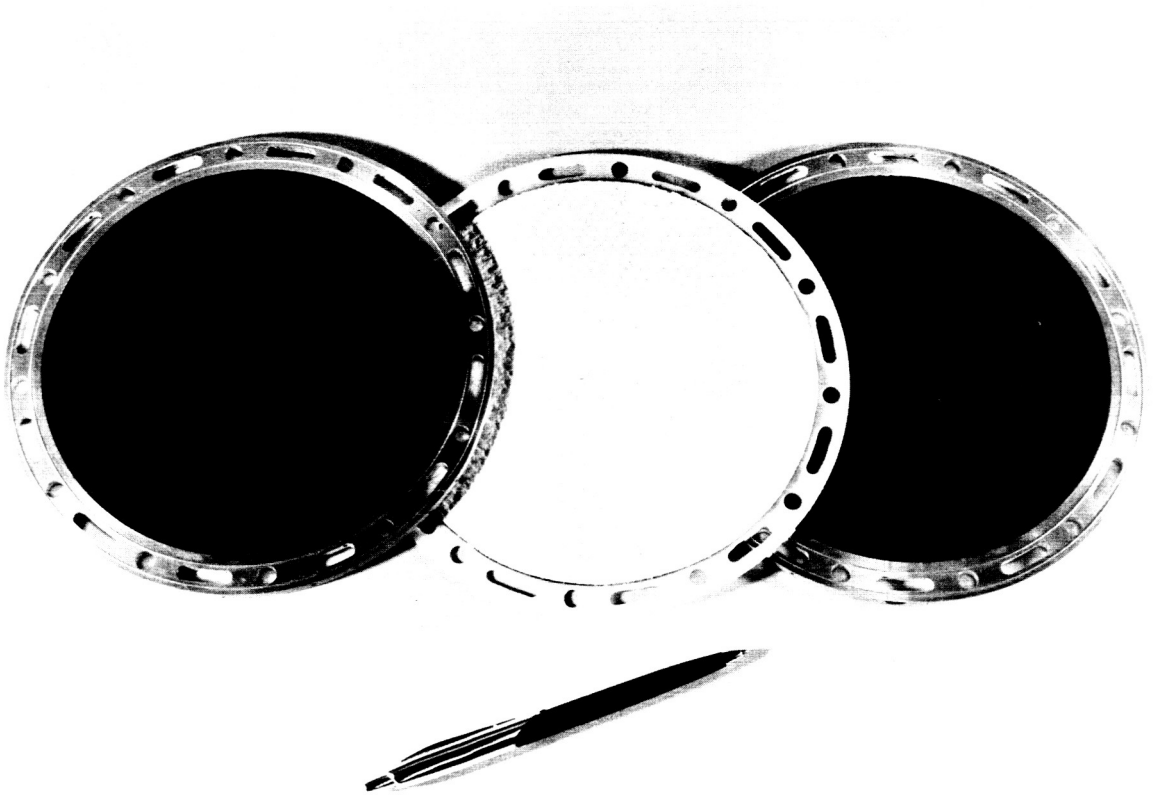

FIG. 4 ELECTRODE AND SEPARATOR OF ASSEMBLY

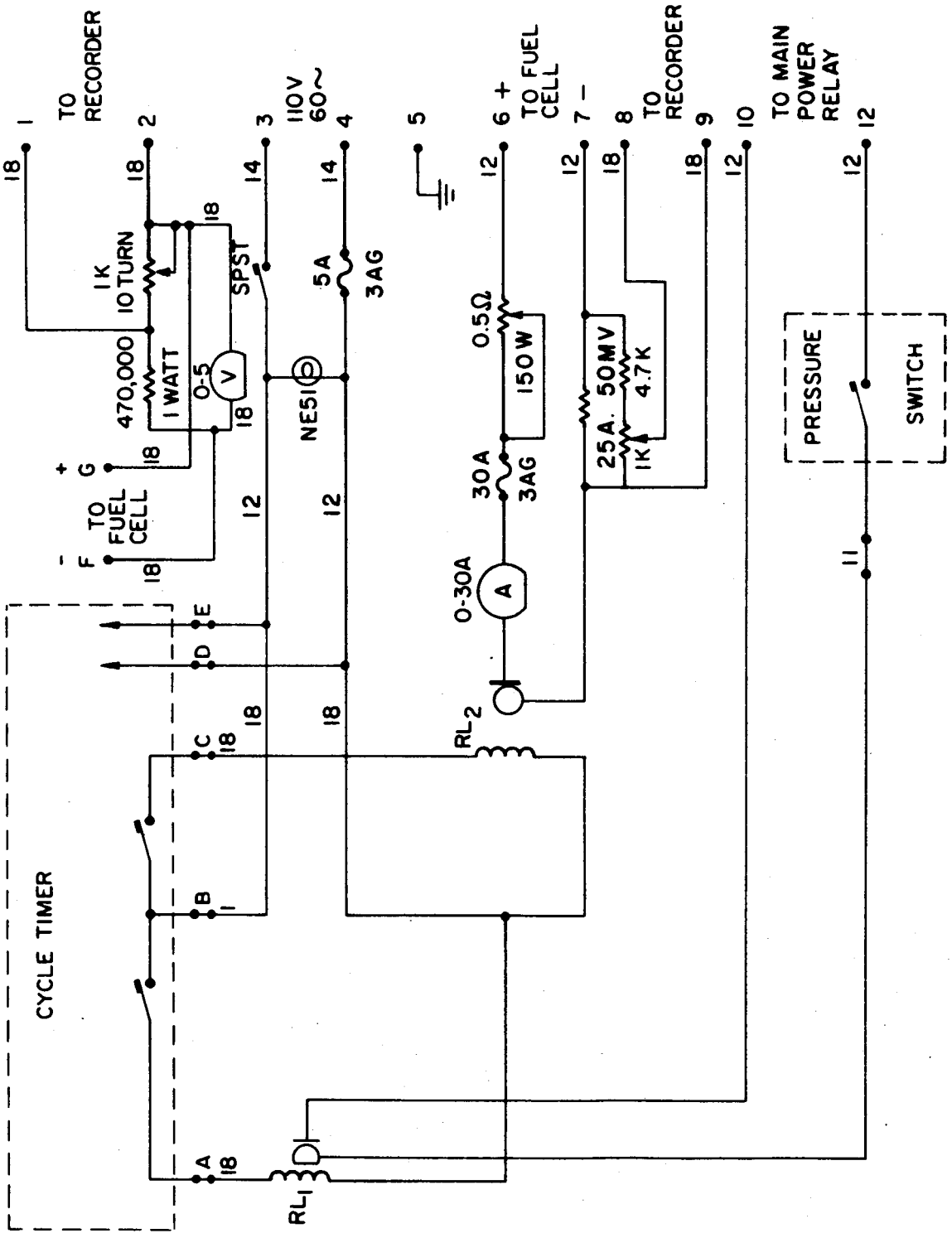

FIG. 5 SCHEMATIC DIAGRAM OF CONTROL APPARATUS

any conventional power supply and multipoint recorder and will automatically cycle and record the performance of the assembly for any given set of charge-discharge conditions.

A tandem recycle timer is employed to switch from charge to discharge and back at the appropriate times. The charge current is set on the power supply,and the discharge current is set by a rheostat within the unit. A voltmeter and ammeter on the unit show the overall assembly voltage and current. Numerous connectors within the unit are employed to transmit the individual cell voltages and temperatures to the channels of the multipoint recorder. A photograph of the power supply, controller and recorder are shown on Figure 6.

3.2 Supporting Developmental Activities

This section presents the results of investigations carried out in support of the fuel cell development.

3.2.1 Single Cell Studies

Single cell tests were carried out in order to confirm the original design estimates on the performance of the final assembly. The components of the single cells employed in these tests were identical to those which will be employed in the final assembly, and the test conditions simulated to those which the final assembly will be subjected. The only difference in the test conditions for the single cell and final assembly was in the manner of storing and applying the gases. For the single cell tests the gases were stored in externally located cylinders whereas in the final assembly the gases will be stored in containers which form an integral part of the assembly. The pressure balance across the cell was maintained manually with the aid of a differential pressure gage in the single cell tests, whereas a flexible diaphragm will be employed to maintain the pressure balance in the final assembly.

The results of these tests are given in Figures 7 and 8. Figure 7 presents the voltage-current characteristics of two

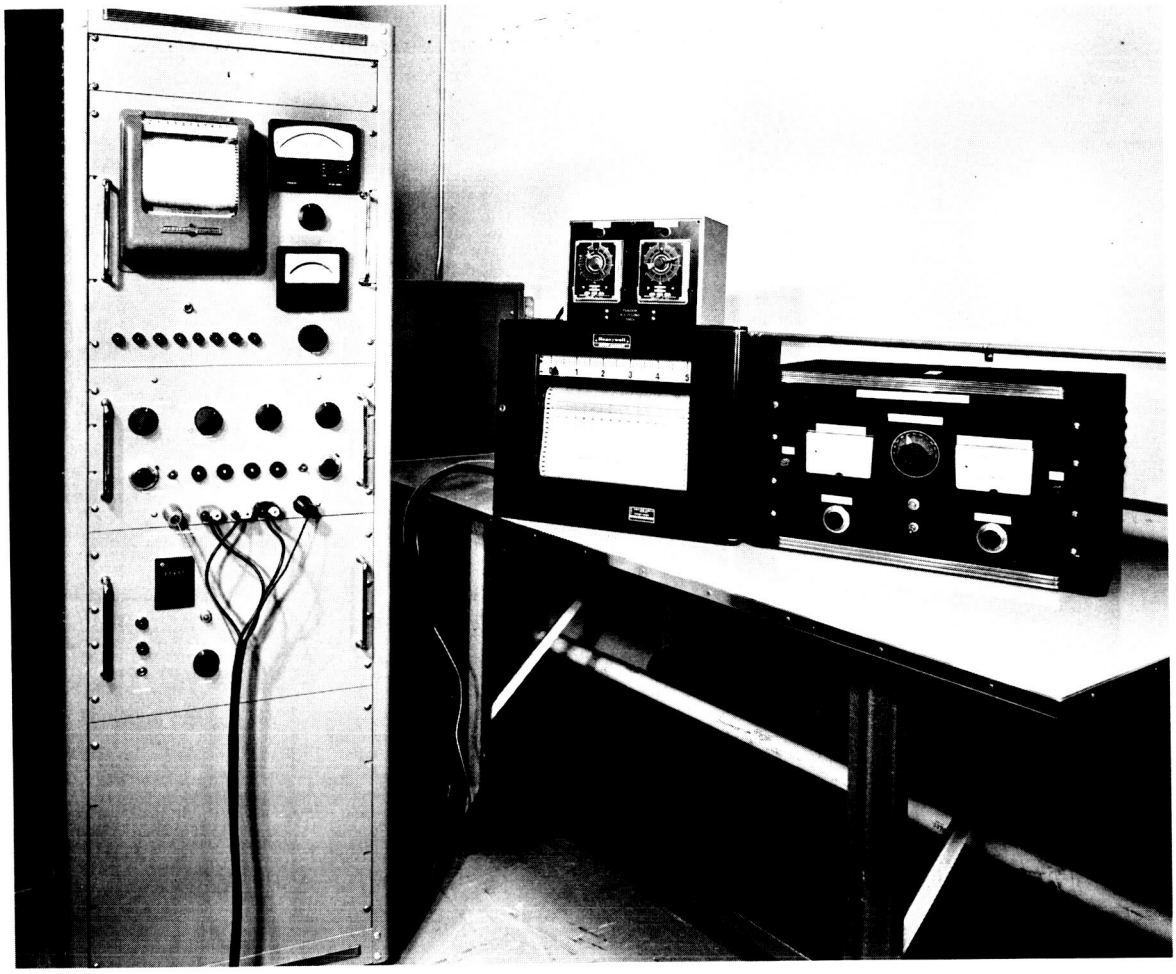

FIG. 6 INSTRUMENT CONTROL AND RECORDING APPARATUS

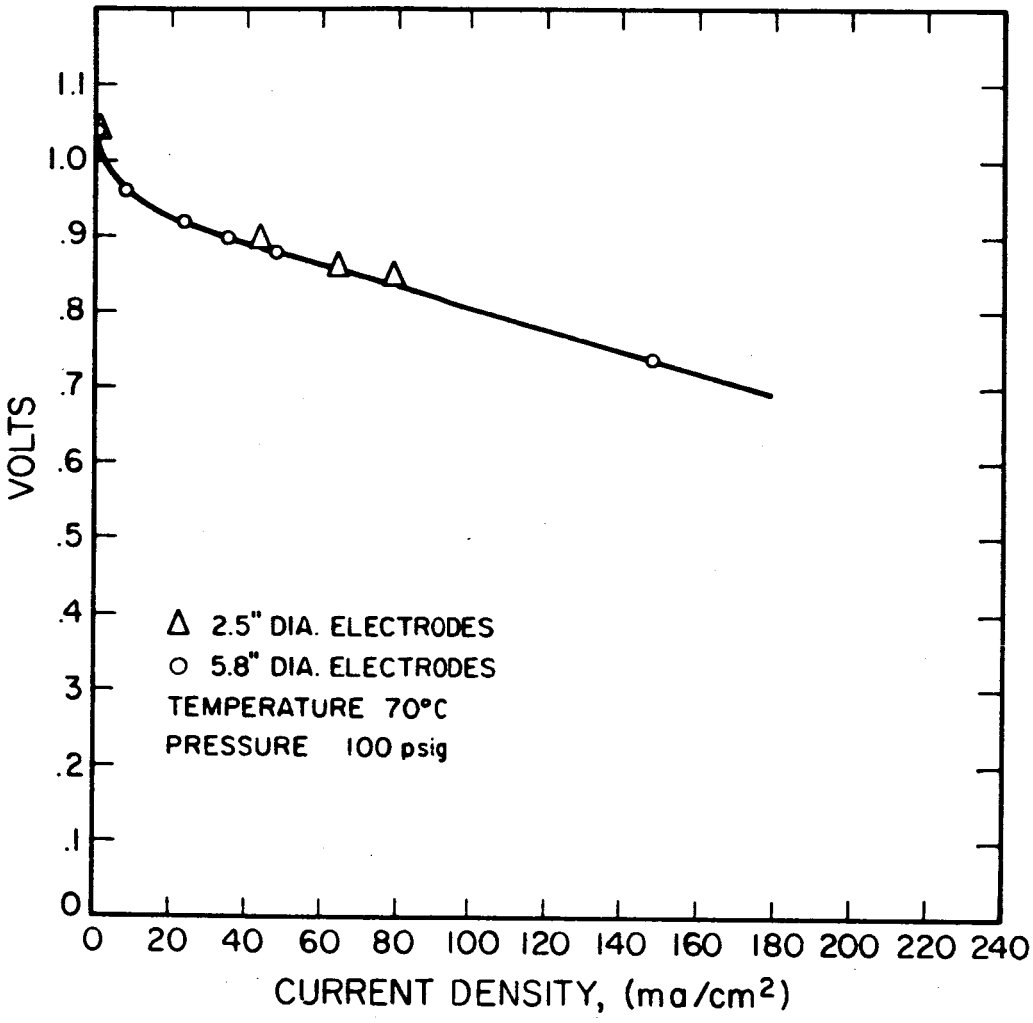

FIG. 7 EFFECT OF ELECTRODE DIAMETER ON VOLTAGE-CURRENT CHARACTERISTICS

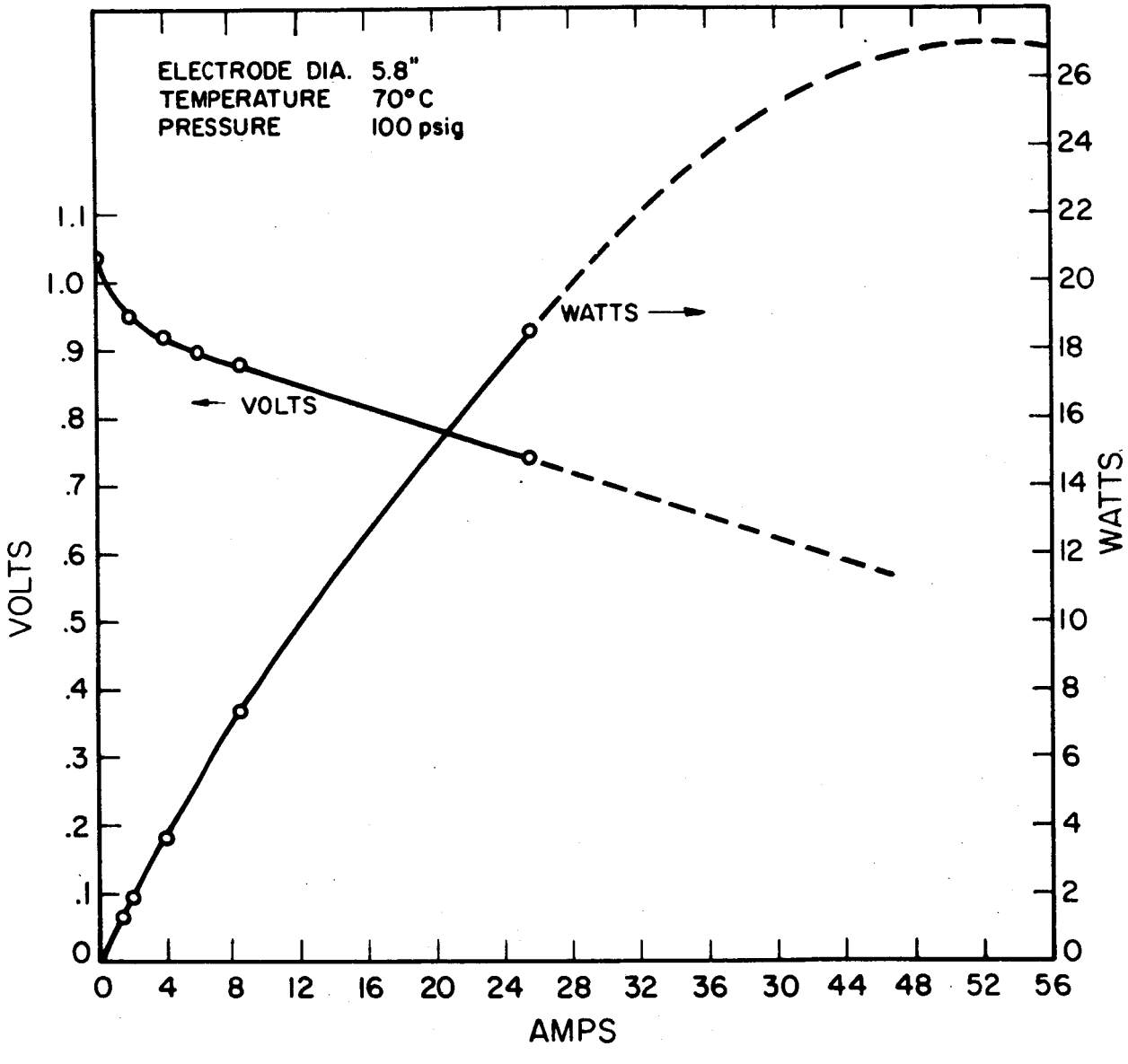

FIG. 8 VOLTAGE CURRENT AND POWER OUTPUT OF PROTOTYPE SINGLE CELL

single cells, one with large, 5.8 inch diameter, and one with small 2 1/2 inch diameter electrodes. The results indicate identical voltage-current density characteristics, and thereby indicate that there are no power losses associated with scaling to electrode diameters of nearly 6 inches, the size to be employed in the final assembly. The results also show that the anticipated current output of slightly over 100 m.a./cm^2 can be obtained at a voltage of 0.8 volts with the large diameter electrodes. This latter result demonstrated that the power output of the final assembly should meet the requirements of 75 watts at a voltage of $\approx$ 5 volts.

The power output of the cell with 5.8 inch diameter electrodes is given as a function of current in Figure 8. The maximum power output is found to be 27 watts at a current of 52 amps. The maximum power output of the final six cell assembly should therefore be approximately 162 watts. For the desired current output of $\approx$ 19 amps, the power output is approximately 14 watts per cell and the output of the final assembly should therefore be $\approx$ 84 watts. (The terminal voltage of the assembly should be 4.4 volts for the latter condition.)

The results of a complete cycle test on one of the smaller single cells is given in Figure 9. The "depth" of the cycle for this run is approximately the same as that depth to which the final assembly will be subjected. The results indicate a relatively constant charge voltage near 1.5 volts at a charge current of 53 m.a./cm^2, and a relatively constant discharge voltage near 0.8 volts at a discharge current of 104 m.a./cm^2. The small drop in voltage at the beginning of the discharge period is attributed to a short term pressure imbalance caused by inadequate control of the manually operated pressure regulators. Disregarding the above pressure effect, it may be said that the cell exhibits fair voltage stability throughout the complete charge-discharge cycle.

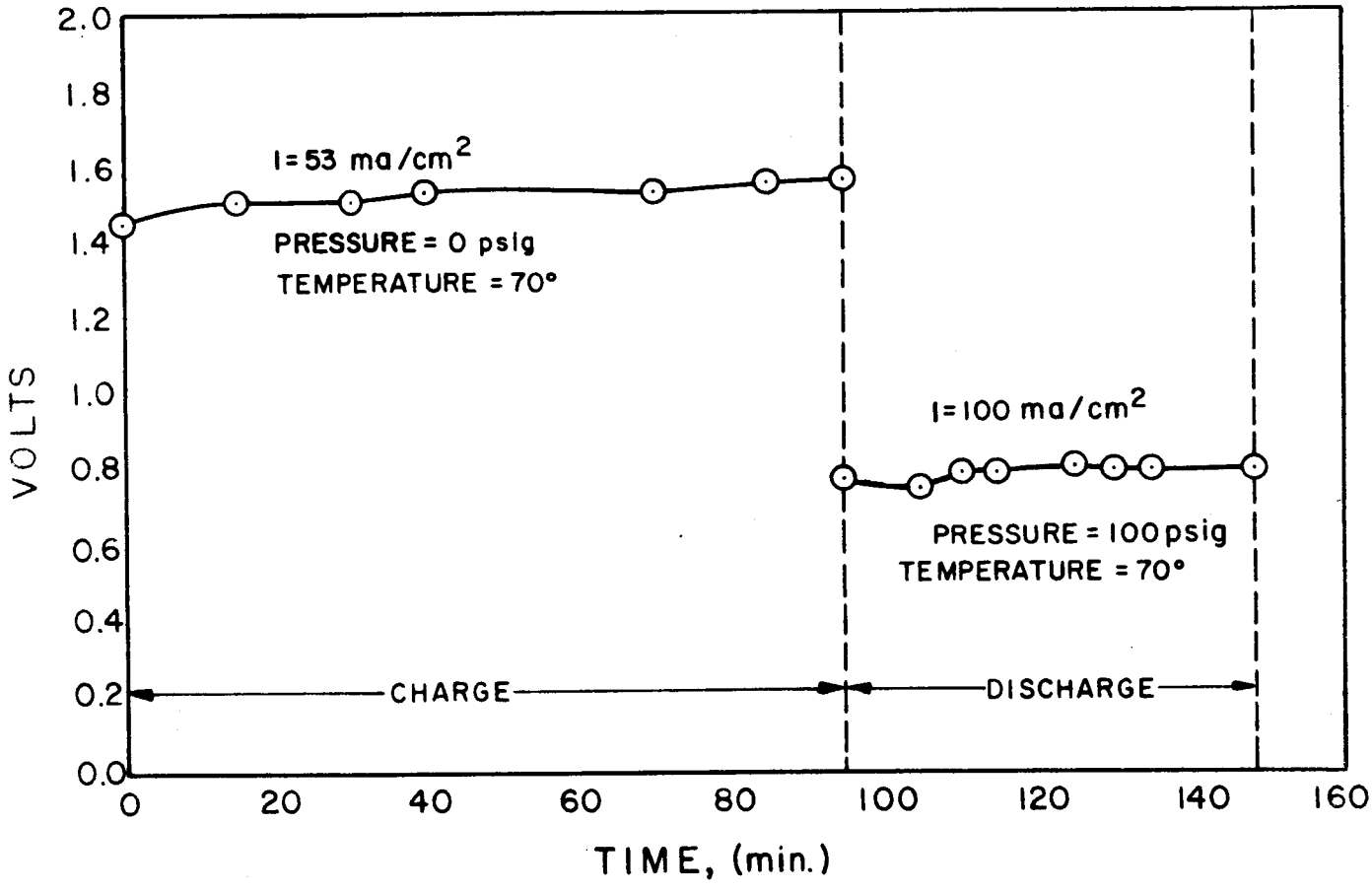

FIG. 9 CHARGE-DISCHARGE CHARACTERISTICS @ 70°C OF A SINGLE CELL

3.2.2 Heat Balance Studies

Heat generation and heat transfer analyses were performed in order to determine the necessity of either supplying external heating or cooling to the assembly for testing within the laboratory (earth environment rather than space environment). The results of these analyses are presented below.

3.2.2.1 Heat Generation

Heat generation within the fuel cell is attributed to two causes; the first is cell polarization, and the second is the entropy change for the hydrogen-oxygen reaction. During discharge, the heat generation rate for a single cell is given by the following relationship:

$$Q = \Delta V \cdot I + T \cdot \Delta S \cdot I \cdot k$$

where

Q = heat generation (watts)

ΔV = polarization loss (volts), equal to the difference between the theoretical open circuit voltage 1.23 volts, and the operating cell voltage, i.e., 0.7 to 1.0 volts.

I = cell current (amps)

T = temperature (^{o}K)

ΔS = entropy change for the hydrogen-oxygen reaction, cal/mol/^{o}K

k = conversion factor to express the second term in the right hand side of the equation in terms of watts. The constant is the product of two other conversion factors which consist of the following:

$$k = \frac{\text{watt-hrs}}{\text{cal}} \times \frac{\text{mols } H_2O}{\text{amp-hr}}$$

$$k = (1.163 \times 10^{-3}) \times (.0189) = 2.2 \times 10^{-5}$$

Based on a single cell performance data, the following values may be substituted in the above equation to obtain the heat generation per cell during discharge at 19 amps and charge at 9.6 amps.

ΔV = 0.43 volts discharge, 0.31 volts charge

I = 19 amps discharge, 9.6 amps charge

T = $70^{\circ}C = 343^{\circ}K$

ΔS = 39 cal/mol$^{\circ}C$

k = 2.2×10^{-5}

The heat generation is thus found to be 13.8 watts for discharge and 0 watts for charge for a single cell. For the six cell assembly the rates will be six times the unit cell rate and correspond to values of 82.8 watts for discharge and again 0 watts for charge.

The rate of heat generation in the six cell assembly has been calculated for other current loads, and the results are given in Figure 10. Inspection of this figure indicates that the heat generation during discharge is always positive and varies in a near linear manner with current. For discharge, however, it is noted that the heat generation is slightly negative at low currents and becomes positive at higher currents. At low charge currents, then it may be said that the assembly will absorb heat from the surroundings.

3.2.2.2 Heat Transfer

For ambient test conditions, heat may be transferred from the assembly by both convection and radiation. The rates of heat transfer by these mechanisms are given by the following equations:

$$Q_C = h\,A\,\Delta t; \quad h = .5\left(\frac{\Delta t}{D}\right)^{.25}$$

$$Q_R = \sigma A \epsilon \left[\left(\frac{T_c + 460}{100}\right)^4 - \left(\frac{T_a + 460}{100}\right)^4\right]$$

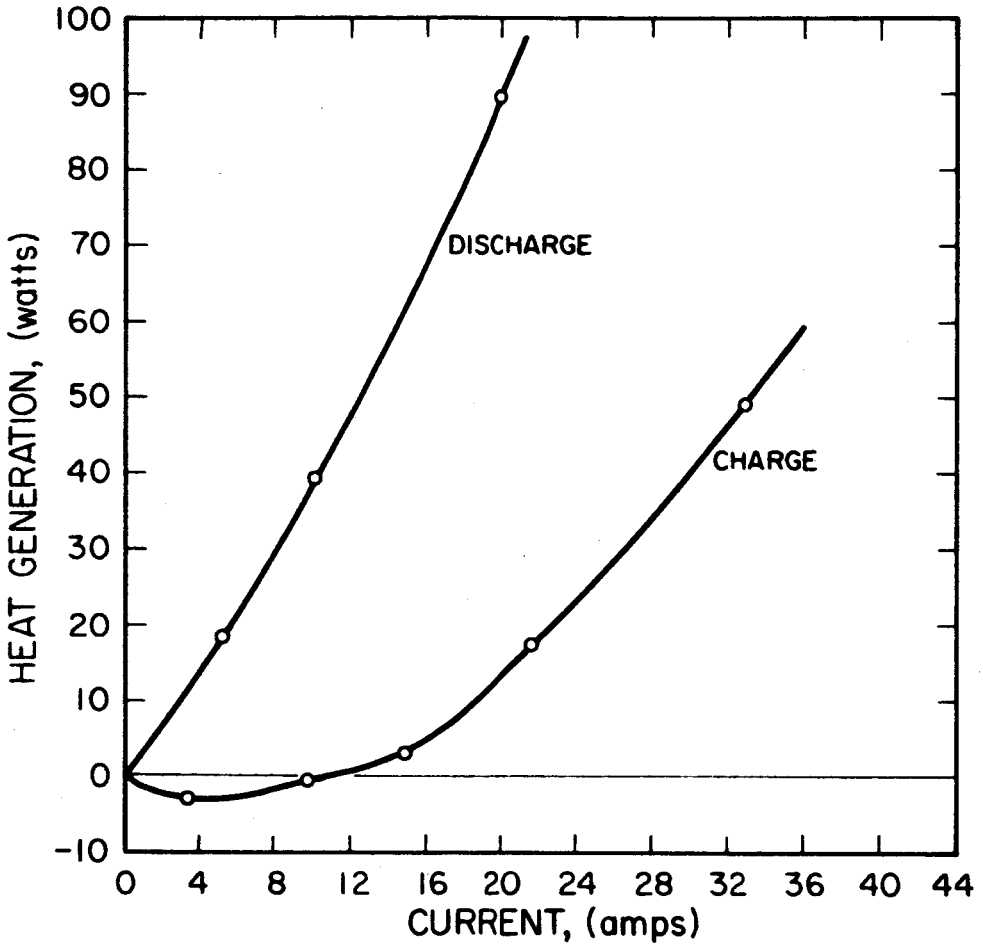

FIG. 10 HEAT GENERATION IN SIX CELL PROTOTYPE

where:

Q_C = heat transfer by natural convection, BTU/hr

h = coefficient of heat transfer, BTU/hr/ft^2/$^\circ$F

A = external surface area of assembly

Δt = temperature difference between assembly and ambient, $^\circ$F

D = diameter of assembly, inches

Q_R = heat transfer by radiation, BTU/hr.

σ = constant, 0.171

ϵ = emissivity

T_c = temperature of assembly, $^\circ$F

T_a = ambient temperature, $^\circ$F

The values of the heat transfer rates by convection and radiation may be calculated on the basis of an assumed ambient temperature of 25°C (76°F) and fuel cell assembly temperature of 70°C (157°F).

$\Delta t = (157-76) = 81^\circ$F

$D = 8$ inches

$\therefore \quad h = 0.5\left(\frac{81}{8}\right)^{.25} = 0.885$

$\therefore \quad Q_c = 0.885 \times 2.47 \times 76 = 177$ BTU/hr = 52 watts

The emissivity can, of course, be varied by application of various types of coatings to the surface of the assembly. The value of the emissivity for an unpolished nickel plated surface (which will be the case if no additional coatings are applied to the assembly) is given as 0.11. The rate of heat transfer by radiation is thus found to be:

$$Q_R = 0.171 \times 2.46 \times 0.11 \left[\left(\frac{617}{100}\right)^4 - \left(\frac{536}{100}\right)^4\right]$$

$$Q_R = 24.5 \frac{\text{BTU}}{\text{hr}} = 7 \text{ watts.}$$

If the assembly is coated with a suitable black paint with emissivity of 0.9, the rate of heat transfer by radiation is found to be 194 BTU/hr or 65 watts.

The total heat transfer from the asembly "Q_T" is equal to the sum of the transfer rates by convection Q_c and radiation Q_R. For the assumed cell and ambient temperatures above, the value of Q_T is found to be 59 watts for $\epsilon = 0.11$ and 127 watts for $\epsilon = 0.9$.

Calculations have also been carried out for the total heat transfer rate at various assumed cell temperatures. The results of these calculations are given in figure 11 for the two assumed emissivities above,and for a fixed ambient temperature of 76°F. If the cycle times were long enough, the results of this graph could be used to estimate the steady state temperature of the fuel cell as a function of load. For example, at a discharge current of 10 amps, the heat generation rate is found to be 40 watts (see figure 10). For an emissivity value of 0.11 the results in figure 11 indicate that the steady state temperature corresponding to a heat dissipation rate of 40 watts is 133°F.

3.2.2.3 Thermal Capacity

The fuel cell assembly contains a quantity of stearic acid which serves as a thermal storage material. The function of the thermal storage medium is to provide for isothermal cell operation during cycling in a space environment. The stearic acid would absorb that fraction of the total heat which is not dissipated by radiation during discharge, and would supply that heat to the cell to balance the radiation losses during charge.

The amount of stearic acid is approximately 30 $inches^3$, and its density is 0.80 gms/cm^3. The weight of stearic acid is therefore 393 gms. The heat of fusion of this material is 47.6 cal/gm and the total thermal capacity is 18,400 cal or the equivalent of 21.4 watt-hrs of electrical energy.

3.2.2.4 Heat Balance

The results of the three preceeding sections may now be employed to estimate the net heat transfer from the fuel cell for the case of cycling at ambient conditions. Let us assume

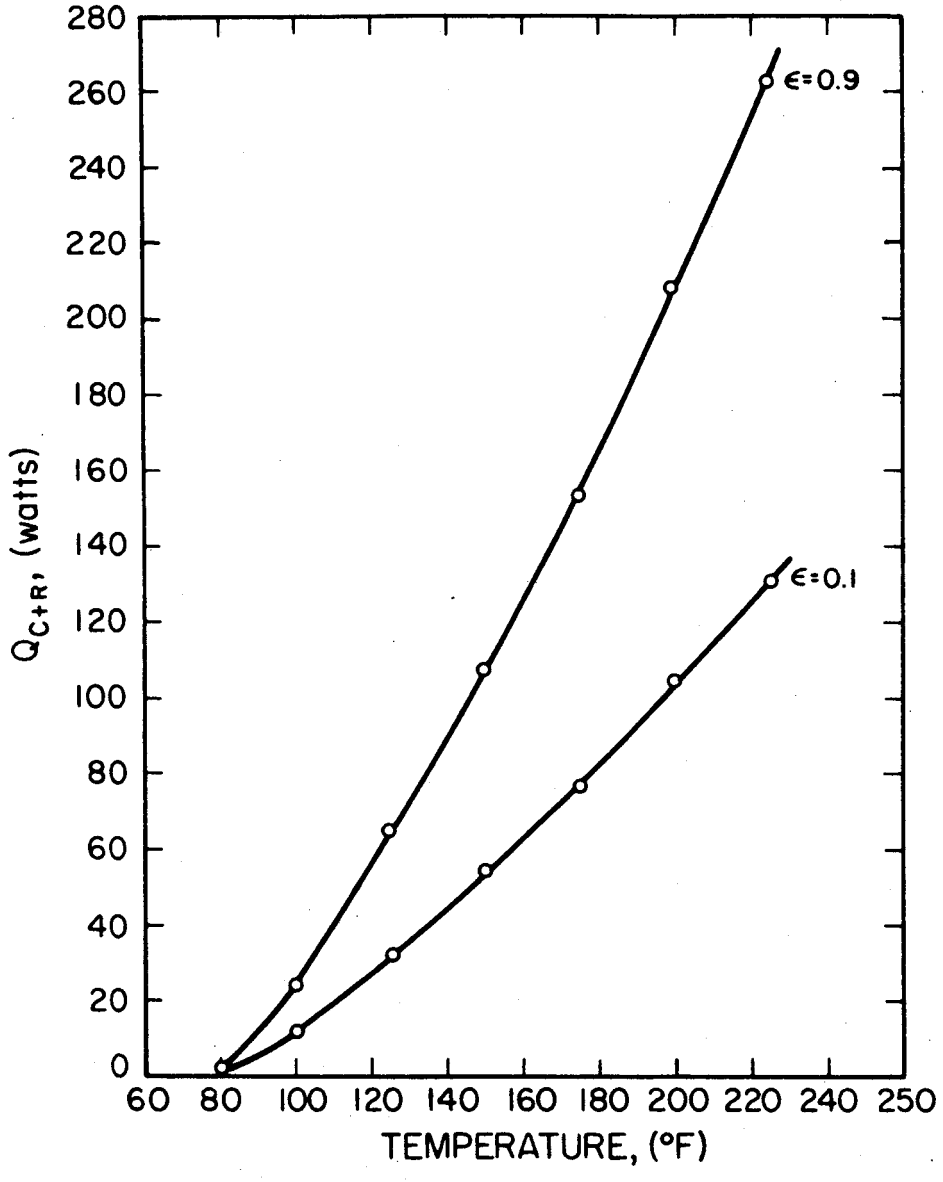

FIG. 11 HEAT TRANSFER FROM SIX CELL PROTOTYPE BY CONVECTION AND RADIATION

that the assembly is initially at 70°C, is uninsulated, that the stearic acid is in the frozen (solid) state, and finally that the cell is fully charged. The net heat transfer for a cycle beginning under these conditions may be determined as follows:

A.	Total cycle time	= 1.890 hrs.
B.	Discharge time	= 0.625 hrs.
C.	Charge time	= 1.265 hrs.
D.	Rate of heat generation during discharge	= 82.8 watts
E.	Rate of heat generation during charge	= 0 watts
F.	Total heat generated during discharge	= 51.7 w-h
G.	Heat absorbed by stearic acid during discharge	= 21.4 w-h
H.	Heat to be rejected during discharge	= 30.3 w-h
I.	Total heat generated during charge	= 0 w-h
J.	Rate of heat transfer by convection	= 52 watts
K.	Heat transfer by convection during discharge	= 32.4 w-h
L.	Heat transfer by convection during charge	= 65.8 w-h
M.	Rate of heat transfer by radiation	= 7 watts (ϵ = 0.11) 57 watts (ϵ = 0.9)
N.	Heat transfer by radiation during discharge	= 4.4 w-h (ϵ = 0.11) 35.6 w-h (ϵ = 0.9)
O.	Heat transfer by radiation during charge	= 8.9 w-h (ϵ = 0.11) 72.0 w-h (ϵ = 0.9)

P.	Heat supplied by stearic acid during charge	= 21.4 w-h
Q.	Total heat rejection during discharge	= 36.8 w-h (ϵ = 0.11) 68.0 w-h (ϵ = 0.9)
R.	Total heat rejection during charge	= 74.7 w-h 137.8 w-h
S.	Net heat lost during discharge	= 6.5 w-h (ϵ = 0.11) 37.7 w-h (ϵ = 0.9)
T.	Net heat lost during charge	= 53.3 w-h (ϵ = 0.11) 116.4 w-h (ϵ = 0.9)

These results indicate a net loss of heat from the assembly during both discharge and charge. For isothermal operation at 70°C under ambient test conditions, it will therefore be necessary to supply additional heat to the assembly or to provide extra insulation. It is anticipated that the heating tapes that will be used to initially heat the cell to 70°C will provide the required extra insulation needed.

3.2.3 Materials Testing

Based on previous experimental results, the most critical materials problem associated with this device is the oxidation of components which are in contact with oxygen, the electrolyte and the electrodes. In this assembly, the metallic parts are made of magnesium and aluminum which are materials that can and would react either chemically or electrochemically with the electrolyte and oxygen if not protected by an inert coating. Therefore, these parts will be plated with a 3 mil layer of nickel, a metal which is chemically inert under these conditions. An additional problem then is to insure that the nickel plate is continuous throughout all surfaces, and of sufficient thickness to adequately protect the magnesium and aluminum from the electrolyte.

Several series of corrosion tests were carried out in order to test the stability of the materials which are to be employed in the final assembly. The first such test consisted of immersing a sample of nickel plated magnesium in a solution of 35 percent KOH solution at 70°C for a period of 7 days. The sample contained a coating of 3 mils of electroless plated nickel. The initial weight and thickness of the sample were 24.1001 gms. and 0.0466 inches respectively, and its surfaces were smooth and shiny. The final weight and thickness were 24.1009 gms. and 0.0468 inches respectively. The surfaces were still smooth, but exhibited a slightly tarnished appearance. There were no signs of penetration of the nickel layer.

Another sample of nickel plated magnesium was subjected to an electrolysis test using conditions similar to the above. In this case, the part was employed as the back up plate for a positive electrode in a single cell assembly. The cell was charged for a total of 24 hours at a current density of 50 m.a./cm^2 at 1.5 volts and at 70°C. As in the above test, the only change in the part was found to be a slight discoloration of the surface. There was no evidence of surface penetration.

A third test was designed to test the stability of the unplated metals, magnesium and aluminum, in a high pressure oxygen environment at elevated temperatures. Samples of magnesium (type AZ231) and aluminum (type 6061) were placed in a container, pressurized to 100 psig with oxygen and held at 100°C for 5 days. The initial and final weights of the magnesium were the same. The initial and final weights of the aluminum were 0.9641 and 0.9642 gms. respectively.

In order to complete the materials evaluation, a fourth and final test was carried out on a sample of butyl rubber, the material of construction for the pressure balance diaphragm. The objective of this test was to determine the stability of this material

in a high pressure oxygen environment at elevated temperatures. The conditions for the test were the same as for the magnesium and aluminum samples, i.e., 100 psig 0_2 at 100°C for 5 days. The initial and final weights of the sample were 0.4729 gms. and 0.4859 gms. respectively. There was no apparent change in surface properties or elasticity. It is not known what caused this weight change, but it is not believed to be critical. It may be surmised that the weight change was caused by oxidation of the sample.

4. FUTURE PLANS

Work during the final quarter of this program will be concentrated on testing the 75 watt model to determine its characteristics as a function of various operating and environmental parameters. It is anticipated that final assembly and initial testing will be started prior to the next monthly reporting period.

5. FINANCIAL STATEMENT

Expenditures for the second quarter were as follows:

Direct Labor Hours	1,233.5
Direct Labor Dollars	$ 5,688.90
Total Expenditures	$18,955.52